

# Novel $J_{eff} = 1/2$ Mott State Induced by Relativistic Spin-Orbit Coupling in $\text{Sr}_2\text{IrO}_4$

B. J. Kim,<sup>1</sup> Hosub Jin,<sup>1</sup> S. J. Moon,<sup>2</sup> J.-Y. Kim,<sup>3</sup> B.-G. Park,<sup>4</sup> C. S. Leem,<sup>5</sup> Jaeju Yu,<sup>1</sup> T. W. Noh,<sup>2</sup> C. Kim,<sup>5</sup> S.-J. Oh,<sup>1</sup> J.-H. Park,<sup>3,4,\*</sup> V. Durairaj,<sup>6</sup> G. Cao,<sup>6</sup> and E. Rotenberg<sup>7</sup>

<sup>1</sup>*CSCMR & School of Physics and Astronomy,  
Seoul National University, Seoul 151-747, Korea*

<sup>2</sup>*ReCOE & School of Physics and Astronomy,  
Seoul National University, Seoul 151-747, Korea*

<sup>3</sup>*Pohang Accelerator Laboratory, Pohang University  
of Science and Technology, Pohang 790-784, Korea*

<sup>4</sup>*eSSC & Department of Physics, Pohang University  
of Science and Technology, Pohang 790-784, Korea*

<sup>5</sup>*Institute of Physics and Applied Physics, Yonsei University, Seoul, Korea*

<sup>6</sup>*Department of Physics and Astronomy,  
University of Kentucky, Lexington, KY 40506*

<sup>7</sup>*Advanced Light Source, Lawrence Berkeley National Laboratory, Berkeley, CA 96720*

## Abstract

We investigated electronic structure of 5d transition-metal oxide  $\text{Sr}_2\text{IrO}_4$  using angle-resolved photoemission, optical conductivity, and x-ray absorption measurements and first-principles band calculations. The system was found to be well described by novel effective total angular momentum  $J_{eff}$  states, in which relativistic spin-orbit (SO) coupling is fully taken into account under a large crystal field. Despite of delocalized Ir 5d states, the  $J_{eff}$ -states form so narrow bands that even a small correlation energy leads to the  $J_{eff} = 1/2$  Mott ground state with unique electronic and magnetic behaviors, suggesting a new class of the  $J_{eff}$  quantum spin driven correlated-electron phenomena.

PACS numbers: 71.30.+h, 79.60.-i, 71.20.-b, 71.70.Ej., 78.70.Dm

Mott physics based on the Hubbard Hamiltonian, which is at the root of various noble physical phenomena such as metal-insulator transitions, magnetic spin orders, high  $T_C$  superconductivity, colossal magneto-resistance, and quantum criticality, has been adopted to explain electrical and magnetic properties of various materials in the last several decades [1, 2, 3, 4, 5, 6]. Great success has been achieved especially in  $3d$  transition-metal oxides (TMOs), in which the  $3d$  states are well localized to yield strongly correlated narrow bands with a large on-site Coulomb repulsion  $U$  and a small band width  $W$ . As predicted, most stoichiometric  $3d$  TMOs are antiferromagnetic Mott insulators [5]. On the other hand,  $4d$  and  $5d$  TMOs were considered as weakly-correlated wide band systems since  $U$  is largely reduced due to delocalized  $4d$  and  $5d$  states [7]. Anomalous insulating behaviors were recently reported in some  $4d$  and  $5d$  TMOs [8, 9, 10, 11, 12], and the importance of correlation effects was recognized in  $4d$  TMOs such as  $\text{Ca}_2\text{RuO}_4$  and  $\text{Y}_2\text{Ru}_2\text{O}_7$ , which were interpreted as Mott insulators near the border line of the Mott criteria, *i.e.*  $U \sim W$  [8, 9]. However, as  $5d$  states are spatially more extended and  $U$  is expected to be further reduced, insulating behaviors in  $5d$  TMOs such as  $\text{Sr}_2\text{IrO}_4$  and  $\text{Cd}_2\text{Os}_2\text{O}_7$  have been puzzling [10, 11].

$\text{Sr}_2\text{IrO}_4$  crystallizes in the  $\text{K}_2\text{NiF}_4$  layered structure as  $\text{La}_2\text{CuO}_4$  and its  $4d$  counterpart  $\text{Sr}_2\text{RhO}_4$  [10, 15]. Considering its odd number of electrons per unit formula ( $5d^5$ ), one expects a metallic state in a naïve band picture. Indeed  $\text{Sr}_2\text{RhO}_4$  ( $4d^5$ ) is a normal metal. Its Fermi surface (FS) measured by the angle resolved photoemission spectroscopy (ARPES) agrees well with the first-principles band calculation results [16, 17]. Since both  $d^5$  systems have identical atomic arrangements with nearly the same lattice constants and bond angles [10, 15], one expects almost the same FS topology.  $\text{Sr}_2\text{IrO}_4$ , however, is unexpectedly an insulator with weak ferromagnetism [10]. At this point, it is natural to consider the spin-orbit (SO) coupling as a candidate responsible for the insulating nature since its energy is much larger than that in  $3d$  and  $4d$  systems. Recent band calculations showed that the electronic states near  $E_F$  can be modified considerably by the SO coupling in  $5d$  systems, and suggest a new possibility of the Mott instability [18]. It indicates that the correlation effects can be important even in  $5d$  TMOs when combined with strong SO coupling.

In this Letter, we show formation of new quantum state bands with effective total angular momentum  $J_{eff}$  in  $5d$  electron systems under a large crystal field, in which the SO coupling is fully taken into account, and also report for the first time manifestation of a novel  $J_{eff} = 1/2$  Mott ground state realized in  $\text{Sr}_2\text{IrO}_4$  by using ARPES, optical conductivity, and x-ray

absorption spectroscopy (XAS) and first-principles band calculations. This new Mott ground state exhibits novel electronic and magnetic behaviors; for examples, spin-orbit integrated narrow bands and an exotic orbital dominated local magnetic moment, suggesting a new class of the  $J_{eff}$  quantum spin driven correlated-electron phenomena.

Single crystals of  $\text{Sr}_2\text{IrO}_4$  were grown by flux method [13]. ARPES spectra were obtained from cleaved surfaces *in situ* under vacuum of  $1 \times 10^{-11}$  Torr at the beamline 7.0.1 of the Advanced Light Source with  $h\nu = 85$  eV and  $\Delta E = 30$  meV. The temperature was maintained at 100 K to avoid charging. The chemical potential  $\mu$  was referred to  $E_F$  of a clean Au electrically connected to the samples. The electronic structure calculations were performed by using first-principles density-functional-theory codes with LDA and LDA +  $U$  methods [14]. The optical reflectivity  $R(\omega)$  was measured at 100 K between 5 meV and 30 eV and the optical conductivity  $\sigma(\omega)$  was obtained by using Kramers-Kronig (KK) transformation. The validity of KK analysis was checked by independent ellipsometry measurements between 0.6 and 6.4 eV. The XAS spectra were obtained at 80 K under vacuum of  $5 \times 10^{-10}$  Torr at the Beamline 2A of the Pohang Light Source with  $\Delta h\nu = 0.1$  eV.

Here we propose a schematic model for emergence of a novel Mott ground state by a large SO coupling energy  $\zeta_{SO}$  as shown in Fig. 1. Under the  $O_h$  site symmetry the  $5d$  states are split into triplet  $t_{2g}$  and doublet  $e_g$  orbital states by the crystal field energy  $10Dq$ . In general,  $4d$  and  $5d$  TMOs have sufficiently large  $10Dq$  to yield  $t_{2g}^5$  low-spin ionic state for  $\text{Sr}_2\text{IrO}_4$ , and thus the system with partially filled wide  $t_{2g}$  band would become a metal (Fig. 1(a)). An unrealistically large  $U \gg W$  could lead to a typical spin  $S = 1/2$  Mott insulator (Fig. 1(b)). However, as  $U$  is expected to be even smaller than that in  $4d$  TMOs, a reasonable  $U$  cannot lead to an insulating state as seen from the fact that  $\text{Sr}_2\text{RhO}_4$  is a normal metal. Now let us take the SO coupling into account. The  $t_{2g}$  states effectively correspond to the orbital angular momentum  $L = 1$  states with  $\psi_{m_l=\pm 1} = \mp(|zx\rangle \pm i|yz\rangle)/\sqrt{2}$  and  $\psi_{m_l=0} = |xy\rangle$ . In the *strong SO coupling limit*, the  $t_{2g}$  band splits into *effective* total angular momentum  $J_{eff} = 1/2$  doublet and  $J_{eff} = 3/2$  quartet bands (Fig. 1(c)). Note that the  $J_{eff} = 1/2$  is energetically higher than the  $J_{eff} = 3/2$ , seemingly against the Hund's rule, since the  $J_{eff} = 1/2$  branches out from the  $J_{5/2}$  ( $5d_{5/2}$ ) manifold due to the large crystal field as depicted in Fig. 1(e). As a result, with four electrons filling up the  $J_{eff} = 3/2$  band and the remaining one in the  $J_{eff} = 1/2$  band, the system is effectively reduced to a half-filled  $J_{eff} = 1/2$  single band system (Fig. 1(c)). The  $J_{eff} = 1/2$  spin-orbit integrated states form

a narrow band so that relatively small  $U$  opens a Mott gap, making it a  $J_{eff} = 1/2$  Mott insulator (Fig. 1(d)). The narrow band width is due to reduced hopping elements of the  $J_{eff} = 1/2$  states with isotropic orbital and mixed spin characters, which are differentiated from the atomic  $J = 1/2$  states as discussed later in detail. The formation of the  $J_{eff}$  bands due to the large  $\zeta_{SO}$  explains why  $\text{Sr}_2\text{IrO}_4$  ( $\zeta_{SO} \sim 0.4$  eV, estimated from the calculation) is insulating while  $\text{Sr}_2\text{RhO}_4$  ( $\zeta_{SO} \sim 0.15$  eV) is metallic.

The  $J_{eff}$  band formation is well-justified in the first principles band calculations on  $\text{Sr}_2\text{IrO}_4$  based on local-density approximation (LDA) as well as LDA +  $U$  with and without including the SO coupling presented in Fig. 2. The LDA result (Fig. 2(a)) yields a metal with a wide  $t_{2g}$  band as shown in Fig. 1a, and the Fermi surface (FS) is nearly identical to that of  $\text{Sr}_2\text{RhO}_4$  [16, 17]. The FS, composed of one-dimensional  $yz$  and  $zx$  bands, is represented by hole-like  $\alpha$  and  $\beta_X$  sheets and an electron-like  $\beta_M$  sheet centred at  $\Gamma$ , X, and M points, respectively [16]. As the SO coupling is included (Fig. 2(b)), the FS becomes rounded but retains the overall topology. Despite small variations in the FS topology, the band structure changes remarkably: Two narrow bands are split off near  $E_F$  from the rest of the bands due to formation of the  $J_{eff} = 1/2$  and  $3/2$  bands as shown in Fig. 1(c). The circular shaped FS reflects the isotropic orbital character of the  $J_{eff} = 1/2$  states.

Such a narrow band near  $E_F$  suggests that a small  $U$  can drive the system to a Mott instability. Indeed, a modest  $U$  value opens up a Mott gap and splits the half-filled  $J_{eff} = 1/2$  band into the upper ( $UHB$ ) and lower Hubbard bands ( $LHB$ ), as presented in Fig. 1(d). The *full* LDA + SO +  $U$  results shown in Fig. 2(c) manifest the  $J_{eff} = 1/2$  Mott state. In comparing the LDA + SO and LDA + SO +  $U$  results (Fig. 2(b),(c)), one can see that the band gap is opened up by simply shifting up the electron-like M sheet and down the hole-like  $\Gamma$  and X sheets, yielding a valence band maxima topology as shown in the left panel of Fig. 2(c). It must be emphasized that *without the SO coupling, LDA +  $U$  alone can not account for the band gap*. In that case, the FS topology changes only slightly from the LDA one, as shown in Fig. 2(d), because  $W$  is so large that the small  $U$  can not play a major role. This result demonstrates that the strong SO coupling is essential to trigger the Mott transition in  $\text{Sr}_2\text{IrO}_4$ , which reduces to a  $J_{eff} = 1/2$  Hubbard system.

The electronic structure predicted by the LDA + SO +  $U$  is borne out by ARPES results presented in Fig. 3. The energy distribution curves (EDCs) near  $\mu$  display dispersive band features, none of which crosses over  $\mu$  as expected in an insulator. Fig. 3(b)-(d) show

intensity maps at binding energies of  $E_B = 0.2, 0.3,$  and  $0.4$  eV, highlighting the evolution of the electronic structure near  $\mu$ . The first valence band maximum ( $\beta_X$ ) appears at the X points (Fig. 3(b)). As  $E_B$  increases (Fig. 3(c),(d)), another band maximum ( $\alpha$ ) appears at the  $\Gamma$  points. The band maxima can also be ascertained in EDCs (Fig. 3(a)). The observed electronic structure agrees well with the LDA + SO +  $U$  results, reproducing the correct valence band maxima topology (see the left panel of Fig. 2(c)). Remarkably, the topmost valence band, which represents the  $J_{eff} = 1/2$  LHB, has a very small dispersion ( $\sim 0.5$  eV) although the  $5d$  states are spatially extended and strongly hybridized with the O  $2p$  states.

The band calculations and ARPES provide solid evidences for the  $J_{eff}$  Mott picture. The unusual electronic character of the  $J_{eff} = 1/2$  Mott state is further confirmed in the optical conductivity [19] and the O  $1s$  polarization dependent XAS. The optical conductivity in Fig. 4(a), which shows an  $\sim 0.1$  eV insulating gap in good agreement with the observed resistivity with an activation energy of 70 meV [20], displays an uncommon double-peak feature with a sharp peak A around 0.5 eV and a rather broad peak B around 1 eV. Considering the delocalized  $5d$  states, it is rather unusual to have such a sharp peak A whose width is much smaller than that of the peaks in  $3d$  TMOs. However, this feature is a natural consequence of the  $J_{eff}$ -manifold Hubbard model as depicted in Fig. 1(d). The transitions within the  $J_{eff} = 1/2$  manifold, from LHB to UHB, and from  $J_{eff} = 3/2$  to the  $J_{eff} = 1/2$  UHB results in the sharp peak A and a rather broad peak B, respectively. A direct evidence of the  $J_{eff} = 1/2$  state comes from the XAS which enables one to characterize the orbital components by virtue of the strict selection rules[21]. The results in Fig. 4(b) show an orbital ratio  $xy : yz : zx = 1 : 1 : 1$  within an estimation error ( $< 10\%$ ) for the unoccupied  $t_{2g}$  state. In the ionic limit, the  $J_{eff} = 1/2$  states are  $|J_{eff} = 1/2, m_{J_{eff}} = \pm 1/2\rangle = (|zx, \pm\sigma\rangle \pm i|yz, \pm\sigma\rangle \mp |xy, \mp\sigma\rangle)/\sqrt{3}$ , where  $\sigma$  denotes the spin state. In the lattice, the inter-site hopping, the tetragonal and rotational lattice distortions, and residual interactions with  $e_g$  manifold could contribute to off-diagonal mixing between the ionic  $J_{eff}$  states. However, the mixing seems to be minimal and the observed isotropic orbital ratio, which is also predicted in the LDA + SO +  $U$ , validates the  $J_{eff} = 1/2$  state.

The  $J_{eff} = 1/2$  Mott state contributes to unusual magnetic behaviors. The total magnetic moment is dominated by the orbital moment. In the ionic limit, the spin state of the  $J_{eff} = 1/2$  state is a mixture of  $\sigma$  (up spin) and  $-\sigma$  (down spin) and yields  $|\langle S_z \rangle| = 1/6$ . Meanwhile the orbital state yields  $|\langle L_z \rangle| = 2/3$ , resulting in twice larger orbital moment

than the spin one, *i.e.*  $|\langle L_z \rangle| = 2|\langle 2S_z \rangle|$ . Note that the  $J_{eff} = 1/2$  is distinguished from the atomic  $J = 1/2$  ( $|L - S|$ ) with  $L = 1$  and  $S = 1/2$  despite the formal equivalence. The  $J = 1/2$  has total magnetic moment  $\langle L_z + 2S_z \rangle = \pm 1/3$  with opposite spin and orbital direction ( $L - S$ ), while the  $J_{eff} = 1/2$  gives  $\langle L_z + 2S_z \rangle = \pm 1$  with parallel one. The  $J_{eff} = 1/2$  ( $|L_{eff} - S|$ ) is exactly analogous to the  $J = 1/2$  ( $|L - S|$ ) with mapping  $L_{eff,z} \rightarrow -L_z$ . This is because the  $J_{eff} = 1/2$  is branched off from the atomic  $J = 5/2$  manifold ( $L + S$ ) by the crystal field, the same reason for the violation of the Hund's rule (Fig. 1(e)). This aspect differentiates 5d TMOs from 3d TMOs described by spin-only moments and also from rare-earth compounds with atomic-like  $J$  states.

The LDA + SO +  $U$  predicts that the magnetic ground state has weak ferromagnetism resulting from canted antiferromagnetic (AFM) order with approximately  $22^\circ$  canting angle in the plane. The predicted local moment at each Ir site is  $0.36 \mu_B$  with  $0.10 \mu_B$  spin and  $0.26 \mu_B$  orbital contributions. This value is only about one-third of the ionic value  $1 \mu_B$  ( $0.33 \mu_B$  from the spin and  $0.67 \mu_B$  from the orbital) for  $J_{eff} = 1/2$  but still retains the respective ratio close to 1:2. This large reduction, however, seems to be natural as it is considered that the Ir 5d orbitals strongly hybridize with neighboring O 2p ones and thus significant parts of the moments are canceled in the AFM order. Indeed,  $\text{Sr}_2\text{IrO}_4$  shows weak ferromagnetism below the Curie temperature with local moment  $\mu_{eff} = 0.5 \mu_B/\text{Ir}$ , about one-third of  $\mu_{eff} = 1.73 \mu_B$  for  $S = 1/2$ , as determined from the magnetic susceptibility above  $T_C$  [13]. It should be noted that the origin of the canted AFM order is different from that in the spin-based Mott insulators, which is attributed to the spin canting due to the Dzyaloshinskii-Moriya (DM) interaction [23], the first order perturbation term of the SO coupling on the S basis states. But the  $J_{eff}$  states, in which the SO coupling is fully included, are free from the DM interaction. Their canted AFM order should be explained by the lattice distortion, and the canting angle is indeed nearly identical to that in the Ir-O-Ir bond [10].

The peculiar electronic and magnetic properties of  $\text{Sr}_2\text{IrO}_4$  can be understood as characteristics of the  $J_{eff} = 1/2$  Mott insulator. In spite of the extended 5d states with a small  $U$ , narrow Hubbard bands with a new quantum number  $J_{eff}$  different from the ordinary atomic  $J$  emerge through the strong SO coupling under the large crystal field. This suggests a new class of materials, namely *spin-orbit integrated narrow band system*. The  $J_{eff} = 1/2$  quantum "spin", which incorporates the orbital degrees of freedom, is expected to bring in new quantum behaviors. Indeed, recent findings show that many iridates display highly

unusual behaviors, for examples, non-Fermi liquid behaviors in SrIrO<sub>3</sub> [22] and a spin liquid ground state in Na<sub>4</sub>Ir<sub>3</sub>O<sub>8</sub> [24]. With the relativistic SO coupling, the system is in a new balance of the spin, orbital, and lattice degrees of freedom. It implies that the underlying physics of 5*d* TMOs is not a simple adiabatic continuation of the 3*d* TMO physics to a small *U* regime and a new paradigm is required for understanding their own novel phenomena. "What novel phenomena emerge in the vicinity of this new Mott insulator?" remains as an open question.

Authors thank T. Arima and H. Takagi for invaluable discussions. This work was supported by MOST/KOSEF through eSSC at POSTECH, CSCMR at SNU, ReCOE Creative Research Initiative Program, under grant R01-2007-000-11188-0, POSTECH research fund, and BK21 program. The work at UK was supported by an NSF grant DMR-0552267. The experiments at ALS and PLS are supported by the DOE Office of Basic Energy Science and in part by MOST and POSTECH, respectively.

---

\* Author to whom all correspondences should be addressed. e-mail: jhp@postech.ac.kr

- [1] N. F. Mott, *Metal-Insulator Transitions* (Taylor and Francis, London/Philadelphia, 1990).
- [2] J. Hubbard, Proc. Roy. Soc. London **A276**, 238 (1963).
- [3] P. Fazekas, *Lecture Notes on Electron Correlation and Magnetism* (World Scientific, Singapore, 1999).
- [4] J. G. Bednorz and K. A. Müller, Z. Phys. B **64** 189 (1986).
- [5] M. Imada, A. Fujimori, and Y. Tokura, Rev. Mod. Phys. **70**, 1039 (1998).
- [6] M. P. A. Fisher and G. Grinstein, Phys. Rev. Lett. **60**, 208 (1988).
- [7] W. D. Ryden and A. W. Lawson, Phys. Rev. B **1**, 1494 (1970).
- [8] S. Nakatsuji and Y. Maeno, Phys. Rev. Lett. **84**, 2666 (2000).
- [9] J. S. Lee *et al.*, Phys. Rev. B **64**, 245107 (2001).
- [10] M. K. Crawford *et al.*, Phys. Rev. B **49**, 9198 (1994).
- [11] D. Mandrus *et al.*, Phys. Rev. B **63**, 195104 (2001).
- [12] R. J. Cava *et al.*, Phys. Rev. B **49**, 11890 (1994); T. Shimura *et al.*, *ibid.* **52**, 9143 (1995).
- [13] G. Cao, J. Bolivar, S. McCall, J. E. Crow, and R. P. Guertin, Phys. Rev. B **57**, R11039 (1998).
- [14] M. J. Han, T. Ozaki, and J. Yu., Phys. Rev. B **73**, 045110 (2006).

- [15] T. Vogt and D. J. Buttrey, *J. Sol. State Chem.* **123**, 186 (1996).
- [16] B. J. Kim *et al.*, *Phys. Rev. Lett.* **97**, 106401 (2006).
- [17] F. Baumberger *et al.*, *Phys. Rev. Lett.* **96**, 246402 (2006).
- [18] D. J. Singh, P. Blaha, K. Schwarz, and J. O. Sofo, *Phys. Rev.* **B65**, 155109 (2002); K. Rossnagel and N. V. Smith, *ibid.* **73**, 073106 (2006); H. J. Xiang and M.-H. Whangbo, *ibid.* **75**, 052407 (2007).
- [19] S. J. Moon *et al.*, *Phys. Rev. B* **74**, 113104 (2006).
- [20] B. J. Kim *et al.*, unpublished.
- [21] T. Mizokawa *et al.*, *Phys. Rev. Lett.* **87**, 077202 (2001); H.-J. Noh *et al.*, *Phys. Rev. B* **72**, 052411 (2005).
- [22] G. Cao *et al.*, *Phys. Rev. B* **76**, 100402(R) (2007).
- [23] I. A. Dzyloshinskii, *J. Phys. Chem. Solids* **4**, 241 (1958); T. Moriya, *Phys. Rev.* **120**, 91 (1960).
- [24] Y. Okamoto, M. Nohara, H. Aruga-Katori, and H. Takagi, *Phys. Rev. Lett.* **99**, 137207 (2007).

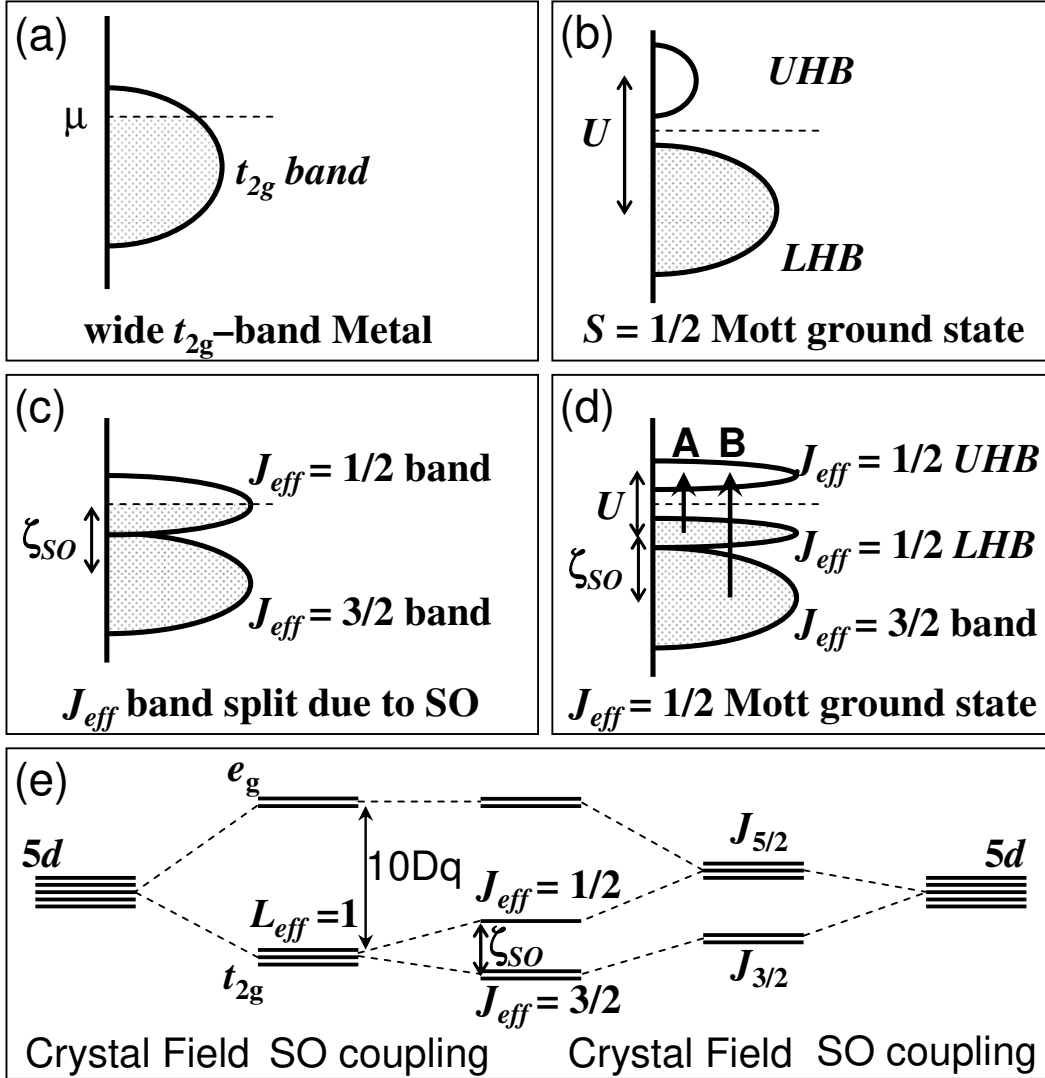


FIG. 1: Schematic energy diagrams for the  $5d^5$  ( $t_{2g}^5$ ) configuration (a) without SO and Hubbard  $U$ , (b) with an unrealistically large  $U$  but no SO, (c) with SO but no  $U$ , and (d) with both SO and  $U$ . Possible optical transitions A and B are indicated by arrows. (e)  $5d$  level splittings by the crystal field and SO coupling.

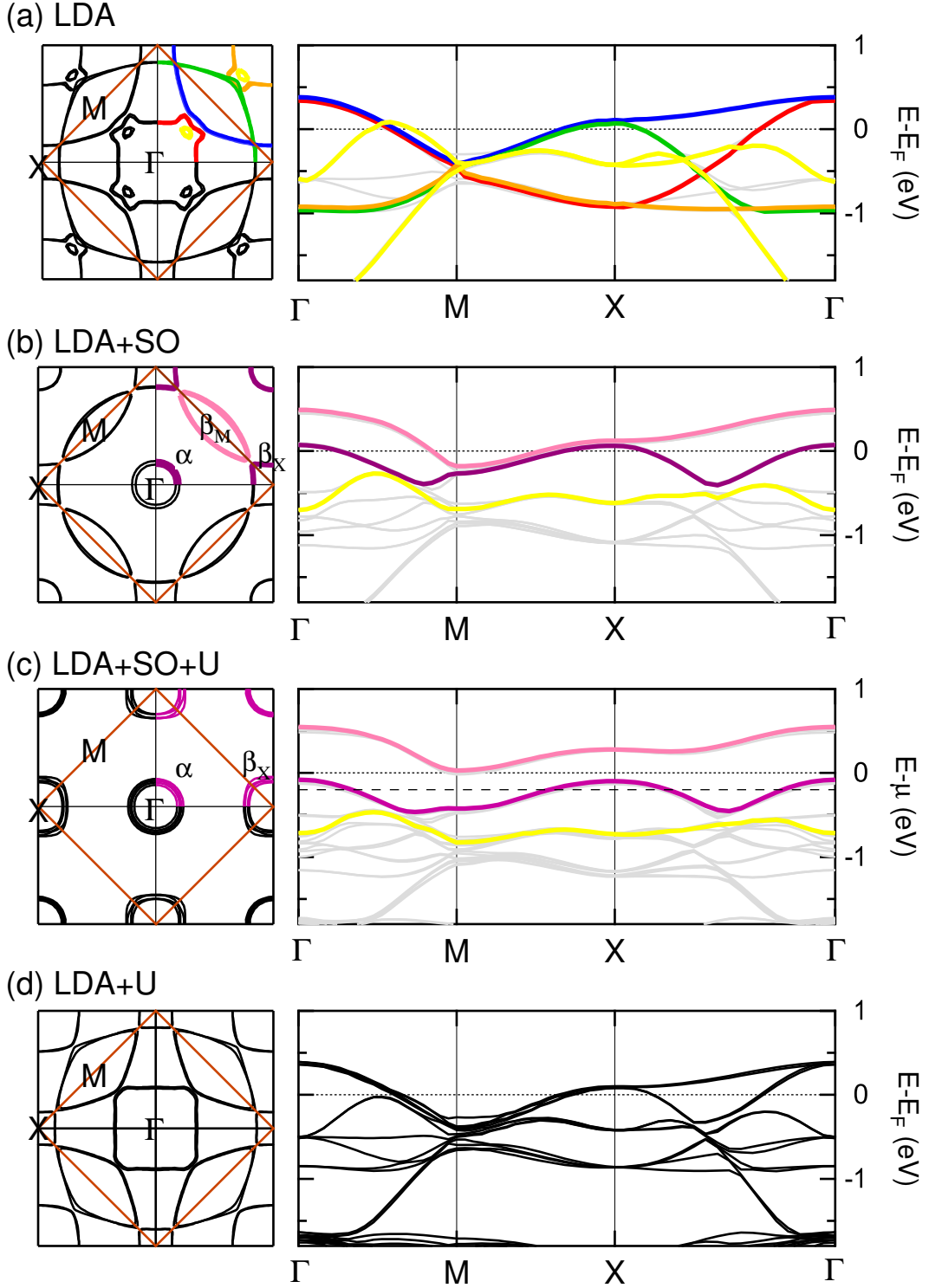


FIG. 2: (Color Online) Theoretical Fermi surfaces and band dispersions in (a) LDA, (b) LDA + SO, (c) LDA + SO +  $U$  (2 eV), and (d) LDA +  $U$ . In (c), the left panel shows topology of valence band maxima ( $E_B = 0.2$  eV) instead of the FS. See the text.

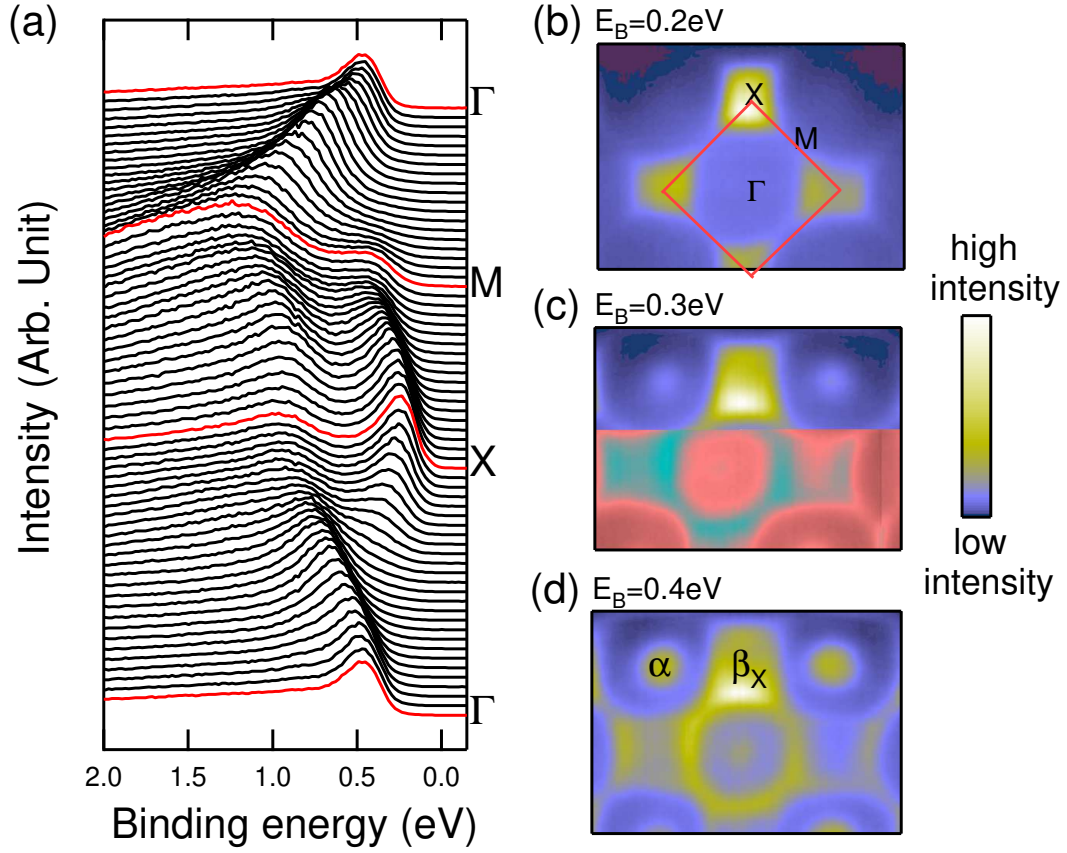


FIG. 3: (Color Online) (a) EDCs up to binding energy  $E_B = 2 \text{ eV}$  along high symmetry lines. (b)-(d) ARPES intensity maps at  $E_B = 0.2 \text{ eV}$ ,  $0.3 \text{ eV}$ , and  $0.4 \text{ eV}$ . Brillouin zone (small square) is reduced from the original one due to the  $\sqrt{2} \times \sqrt{2}$  distortion.

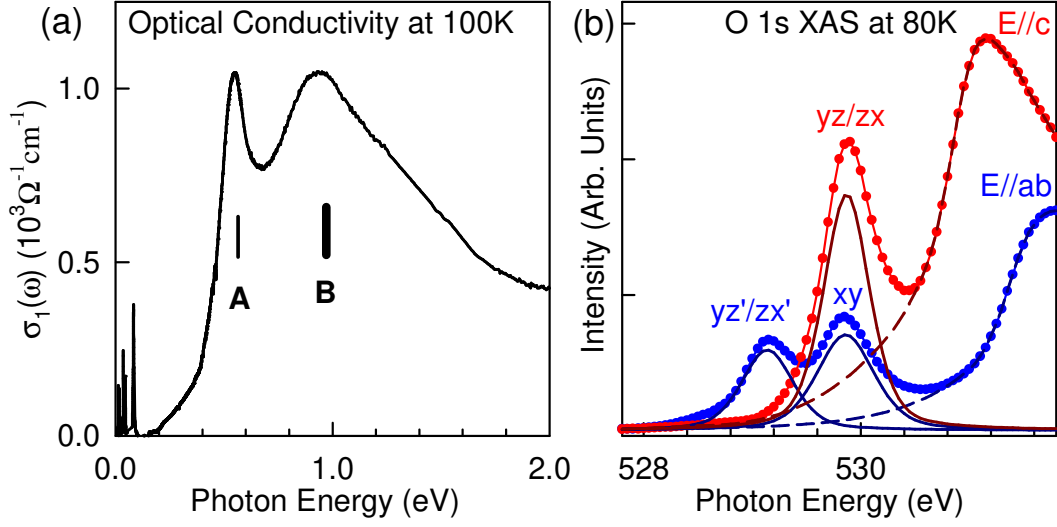


FIG. 4: (Color Online) (a) Optical conductivity. Peak A and B corresponds to transitions denoted in Fig. 1(d). (b) The O 1s polarization dependent XAS spectra (dotted lines) compared with expected spectra (solid lines) under an assumption of  $xy:yz:zx = 1:1:1$  ratio.  $xy$  and  $yz/zx$  denote transitions from in-plane oxygens while  $yz'/zx'$  from apical oxygens, and the energy difference corresponds to their different O 1s core-hole energies [21].